NJC

Accepted Manuscript

This is an *Accepted Manuscript*, which has been through the Royal Society of Chemistry peer review process and has been accepted for publication.

Accepted Manuscripts are published online shortly after acceptance, before technical editing, formatting and proof reading. Using this free service, authors can make their results available to the community, in citable form, before we publish the edited article. We will replace this *Accepted Manuscript* with the edited and formatted *Advance Article* as soon as it is available.

You can find more information about *Accepted Manuscripts* in the Information for Authors.

Please note that technical editing may introduce minor changes to the text and/or graphics, which may alter content. The journal's standard Terms & Conditions and the Ethical guidelines still apply. In no event shall the Royal Society of Chemistry be held responsible for any errors or omissions in this *Accepted Manuscript* or any consequences arising from the use of any information it contains.

ROYAL SOCIETY OF CHEMISTRY

www.rsc.org/njc

Major Differences Between Trifluorophosphine and Carbonyl Ligands in Binuclear Cyclopentadienyliron Complexes

Shida Gong, Qiong Luo, Qian-shu Li, Yaoming Xie, R. Bruce King, and Henry F. Schaefer III

Graphical Abstract

No low-energy $Cp_2Fe_2(PF_3)_n$ structures have bridging PF_3 ligands. Bridging μ-PF_2 groups are found combined with terminal F or PF_4 ligands.

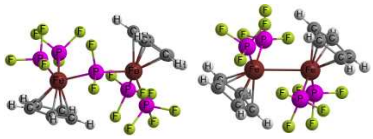

$Cp_2Fe_2(PF_3)_5$ $Cp_2Fe_2(PF_3)_4$

Major Differences Between Trifluorophosphine and Carbonyl Ligands in Binuclear Cyclopentadienyliron Complexes

Shida Gong,[a] Qiong Luo,*[,a] Qian-shu Li,[a] Yaoming Xie,[b] R. Bruce King,*[,a,b] and Henry F. Schaefer III[b]

[a] MOE Key Laboratory of Theoretical Chemistry of Environment, Center for Computational Quantum Chemistry, South China Normal University, Guangzhou 510631, P. R. China

[b]Department of Chemistry and Center for Computational Chemistry, University of Georgia, Athens, Georgia 30602, USA

Abstract

The cyclopentadienyliron trifluorophosphine hydride $CpFe(PF_3)_2H$, in contrast to $CpFe(CO)_2H$, is a stable compound that can be synthesized by reaction of $Fe(PF_3)_5$ with cyclopentadiene. Theoretical studies on the binuclear $Cp_2Fe_2(PF_3)_n$ (n = 5, 4, 3, 2) derivatives derived from $CpFe(PF_3)_2H$ indicate the absence of viable structures having PF_3 ligands bridging Fe-Fe bonds solely through the phosphorus atom. This contrasts with the analogous $Cp_2Fe_2(CO)_n$ systems for which the lowest energy structures have two (for n = 4 and 2) or three (for n = 3) CO groups bridging an iron-iron bond. Higher energy singlet $Cp_2Fe_2(PF_3)_3$ structures have a novel four-electron donor bridging η^2-μ-PF_3 ligand bonded to one iron atom through its phosphorus atom and to the other iron atom through a fluorine atom. Other higher energy triplet and singlet $Cp_2Fe_2(PF_3)_2$ structures are of the $Cp_2Fe_2F_2(\mu\text{-}PF_2)_2$ type having terminal fluorine atoms and bridging μ-PF_2 ligands. The lowest energy $Cp_2Fe_2(PF_3)_5$ structure is actually $Cp_2Fe_2(PF_3)_3(PF_4)(\mu\text{-}PF_2)$ with a bridging PF_2 group and a terminal PF_4 group. Such structures are derived from a $Cp_2Fe_2(PF_3)_4(\mu\text{-}PF_3)$ precursor by migration of a fluorine atom from the bridging PF_3 group to a terminal PF_3 group with a low activation energy barrier.

1. Introduction

The chemistry of cyclopentadienyliron carbonyls dates back approximately 50 years to the synthesis of $Cp_2Fe_2(CO)_4$ by Piper and Wilkinson in 1956 using the simple thermal reaction of $Fe(CO)_5$ with cyclopentadiene dimer (Figure 1: Cp = η^5-C_5H_5).[1] The ready availability of $Cp_2Fe_2(CO)_4$ from inexpensive starting materials has made it a very useful reagent for the synthesis of a variety of important organoiron derivatives. Subsequent determination of the structures of both the *cis* and *trans* stereoisomers of $Cp_2Fe_2(CO)_4$ by X-ray and neutron diffraction confirmed the presence of two bridging CO groups originally suggested by its infrared ν(CO) frequencies.[2,3,4] The Fe–Fe distance of 2.54 Å was consistent with the formal single bond required to give each iron atom the favored 18-electron configuration. Numerous substituted $Cp_2Fe_2(CO)_4$ derivatives are known in which one or more hydrogen atoms of the Cp rings have been replaced by organic groups. All of these substituted derivatives have two bridging CO groups similar to the parent $Cp_2Fe_2(CO)_4$ [= $Cp_2Fe_2(CO)_2(\mu\text{-}CO)_2$].

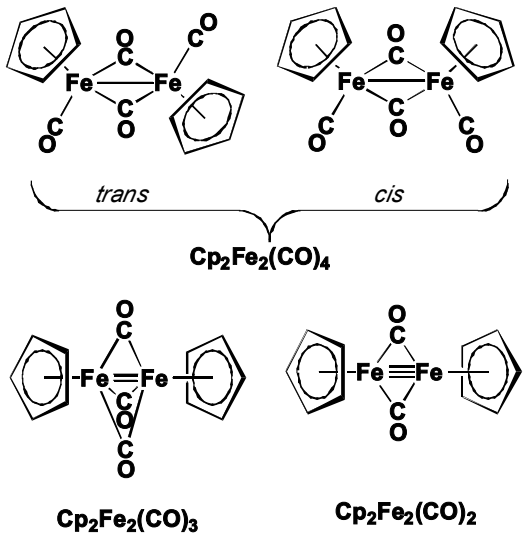

Figure 1. Structures of binuclear cyclopentadienyliron carbonyl derivatives $Cp_2Fe_2(CO)_n$ (n = 4, 3, 2). The compounds $Cp_2Fe_2(CO)_4$ (*cis* and *trans* isomers) and $Cp_2Fe_2(CO)_3$ have been synthesized and structurally characterized by X-ray crystallography. The doubly bridged $Cp_2Fe_2(\mu\text{-}CO)_2$ structure is predicted by density functional theory and is a presumed intermediate in the pyrolysis of $Cp_2Fe_2(CO)_4$ to give $Cp_4Fe_4(\mu_3\text{-}CO)_4$.

Some unsaturated $Cp_2Fe_2(CO)_n$ derivatives are known as isolable compounds (n = 3) or probable reaction intermediates (n = 2) (Figure 1). Photolysis of $Cp_2Fe_2(CO)_4$ gives the triply bridged tricarbonyl $Cp_2Fe_2(\mu\text{-}CO)_3$, which is of interest in being a stable triplet state organometallic molecule.[5,6,7] X-ray crystallography on the corresponding

permethylated derivative (η^5-$Me_5C_5)_2Fe_2(CO)_3$ confirms the presence of three bridging CO groups and indicates a short Fe=Fe distance of 2.265 Å consistent with the formal double bond required to give both iron atoms the favored 18-electron configuration.[8] Some evidence has been presented for the existence of an unbridged isomer of $Cp_2Fe_2(CO)_2$ as a photolysis product of $Cp_2Fe_2(CO)_4$ in low-temperature matrices.[9] However, this is questionable since a theoretical study on $Cp_2Fe_2(CO)_2$ predicts a doubly bridged structure and a very short Fe≡Fe distance of 2.17 Å consistent with the formal triple bond required to give each iron atom the favored 18-electron configuration.[10] The dicarbonyl $Cp_2Fe_2(CO)_2$ is a likely intermediate in the preparation of the very stable tetrahedral iron cluster $Cp_4Fe_4(CO)_4$ by the pyrolysis of $Cp_2Fe_2(CO)_4$ in a solvent such as toluene.[11]

The trifluorophosphine (PF_3) ligand forms complexes closely related to metal carbonyls owing to the strong electron-withdrawing properties of the three highly electronegative fluorine atoms. [12,13,14,15,16,17,18,19,20,21] As a result PF_3, like CO, stabilizes low formal oxidation states so that many binary zerovalent $M(PF_3)_n$ derivatives with terminal PF_3 groups are relatively thermally and oxidatively stable.[22,23,24,25,26,27,28,29] However, known compounds with PF_3 ligands bridging a pair of metal atoms analogous to the numerous metal carbonyls with bridging CO groups are very rare even though compounds with μ_3-PF_3 ligand bridging *three* Pd atoms were reported in the 1990s.[30,31] Nevertheless, Werner and co-workers have synthesized binuclear rhodium complexes containing bridging tertiary phosphine ligands.[32,33,34] Furthermore, theoretical studies on binuclear $M_2(PF_3)_n$ systems show most structures with bridging PF_3 groups to be energetically disfavored relative to isomeric structures with exclusively terminal PF_3 groups.[35,36,37,38] These considerations make of interest the chemistry of $Cp_2Fe_2(PF_3)_n$ derivatives (n = 4, 3, 2) analogous to the $Cp_2Fe_2(CO)_n$ derivatives with two or three bridging CO groups discussed above. We now report theoretical studies that predict totally different preferred structures and energetics for the $Cp_2Fe_2(PF_3)_n$ systems relative to their carbonyl analogues $Cp_2Fe_2(CO)_n$. In particular, the energetically preferred $Cp_2Fe_2(PF_3)_n$ (n = 4, 3, 2) structures reflect the reluctance of PF_3 groups to bridge two metal atoms. Instead PF_3 groups remain in terminal positions in the lowest energy $Cp_2Fe_2(PF_3)_n$ structures. Higher energy $Cp_2Fe_2(PF_3)_n$ structures (n = 4, 3, 2) exhibit interesting novel features such as bridging PF_3 groups of a different type bonded to one iron atom through the phosphorus atom and to the other iron atom through a fluorine lone pair. Examples of a PF_3 group splitting into a bridging PF_2 group and a fluorine atom are also found.

The compounds discussed in this paper are currently unknown but are potentially accessible experimentally. Kruck and Knoll[39] have synthesized $(\eta^4\text{-}C_5H_6)Fe(PF_3)_3$ by the ultraviolet irradiation of $Fe(PF_3)_5$ with cyclopentadiene in diethyl ether (Figure 2). Treatment of $(\eta^4\text{-}C_5H_6)Fe(PF_3)_3$ with triethylamine results in hydrogen migration from carbon to iron to give the hydride $CpFe(PF_3)_2H$, which is a potential precursor to the species discussed in this paper by dehydrogenation under mild conditions (Figure 2).

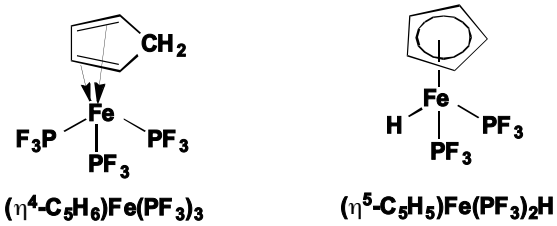

$(\eta^4\text{-}C_5H_6)Fe(PF_3)_3$ $(\eta^5\text{-}C_5H_5)Fe(PF_3)_2H$

Figure 2. The species $(\eta^4\text{-}C_5H_6)Fe(PF_3)_3$ and $CpFe(PF_3)_2H$ synthesized by Kruck and Knoll from $Fe(PF_3)_5$ and cyclopentadiene.

2. Theoretical Methods

Electron correlation effects were considered using density functional theory (DFT) methods, which have evolved as a practical and effective computational tool, especially for organometallic compounds.[40,41,42,43,44,45,46] Three DFT methods were used in this study. The popular B3LYP method combines the three-parameter Becke functional[47] with the Lee-Yang-Parr generalized gradient correlation functional.[48] The BP86 method combines Becke's 1988 exchange functional[49] with Perdew's 1986 gradient corrected correlation functional.[50] Reiher and coworkers have found that B3LYP always favors the high-spin state and BP86 favors the low-spin state for a series of the Fe(II)-S complexes.[51] This is also true for the molecules studied in the present paper so that these two DFT methods may predict the global minima in different spin states. The high-low spin energy difference is a challenge for current DFT approximations,[52,53,54,55,56] and it is found sensitive to the percentage of Hartree-Fock (HF) exchange.[52] For this reason, Reiher and coworkers have proposed a new parametrization for the B3LYP functional, namely B3LYP*, which, by reducing the exact exchange from 20% to 15%, provides electronic state orderings in agreement with experiment. These same authors obtain satisfactory results using the B3LYP* functional on the G2 test set.[57] In the present study, we also adopted the B3LYP* method to give more reliable energy differences among various spin states (singlet, triplet, and quintet). Thus, in order to have a conclusive energy ordering, we mainly discuss the B3LYP* geometries and energies in the text. The corresponding results from the B3LYP and BP86 methods are provided in the Supporting Information.

Double-ζ plus polarization (DZP) basis sets were used for the present study. For hydrogen and the first row atoms carbon and fluorine, one set of p polarization functions, $\alpha_p(H) = 0.75$, and one set of pure spherical harmonic d functions with orbital exponents $\alpha_d(C) = 0.75$ and $\alpha_d(F) = 1.0$, respectively, were added to the standard Huzinaga--Dunning contracted DZ sets,[58] designated as (4s1p/2s1p) for hydrogen and (9s5p1d/4s2p1d) for carbon and fluorine. For phosphorus, an additional set of pure spherical harmonic d functions with orbital exponents $\alpha_d(P) = 0.60$, designated (12s8p1d/6s4p1d), was used.[59] The loosely contracted DZP basis set for iron, was the Wachters' primitive set[60] augmented by two sets of p functions and one set of d functions, and contracted following Hood, Pitzer, and Schaefer designated as (14s11p6d/10s8p3d).[61] For $Cp_2Fe_2(PF_3)_5$, $Cp_2Fe_2(PF_3)_4$, $Cp_2Fe_2(PF_3)_3$, and $Cp_2Fe_2(PF_3)_2$, there are 638, 570, 502, and 434 contracted Gaussian functions, respectively, with the present DZP basis set.

The optimizations and frequency analyses were carried out analytically using the Gaussian 09 program package (B01 version).[62] Analyses of the natural population and Wiberg bond indices were carried out using the Gaussian 03 program package (C02 version).[63] The fine grid (75, 302) was the default for the numerical evaluation of the integrals, while the finer grid (120, 974) was only used to evaluate the small imaginary vibrational frequencies.[64,65,66] The BP86 method was reported to give vibrational frequencies closer to the experiments without using any scaling factors.[67,68] This concurrence may be accidental, since the theoretical vibrational frequencies predicted by BP86 are harmonic frequencies, whereas the experimental fundamental frequencies are anharmonic. However, the discussions about the frequencies are mainly based on the BP86 results. The vibrational frequencies predicted by the three methods are listed in the Supporting Information.

A given $Cp_mFe_2(PF_3)_n$ (**m** = 1, 2; **n** = 2, 3, 4, 5) structure is designated as **mn-aX**, where **a** orders the structure according to their relative energies by the B3LYP* method, and **X** indicates the spin state as **S** (singlet), **D** (doublet), **T** (triplet), or **Q** (quintet for binuclear structures or quartet for mononuclear structures). Consequently, the lowest energy singlet structure for $Cp_2Fe_2(PF_3)_2$ is designated **22-1S**.

3. Results

3.1 Molecular structures

3.1.1 $Cp_2Fe_2(PF_3)_5$. Singlet and triplet structures were both studied for the binuclear $Cp_2Fe_2(PF_3)_5$ derivatives. However, only the four singlet structures, **25-1S** to **25-4S**, were found, since all of the triplet binuclear $Cp_2Fe_2(PF_3)_5$ structures investigated

dissociated into mononuclear fragments. The four lowest energy $Cp_2Fe_2(PF_3)_5$ structures can be classified into two *cis/trans* isomer pairs (Figure 3). The first *cis/trans* pair includes the global minimum **25-1S** (*trans*) and the structure **25-4S** (*cis*) lying 12.1 kcal/mol in energy above **25-1S**. In these two structures, a PF_2 group bridges $CpFe(PF_3)_2$ and $CpFe(PF_3)(PF_4)$ fragments. This pair of structures can be generated by transfer of a fluorine from a bridging PF_3 group to a terminal PF_3 group to give a bridging PF_2 group and a terminal PF_4 group. The other *cis/trans* isomer pair includes the C_1 structure **25-2S** and the C_2 structure **25-3S**, which lie 7.5 and 9.7 kcal/mol, respectively, in energy above **25-1S**, respectively. In this pair, the bridging PF_3 group connects two $CpFe(PF_3)_2$ fragments.

All four singlet $Cp_2Fe_2(PF_3)_5$ structures thus consist of two mononuclear units connected solely by a bridging PF_2 or PF_3 group. The relatively long Fe-Fe distances (> 4.0 Å) and the low Wiberg bond indices (WBIs) of the Fe-Fe bond (< 0.05) (Table 1) confirm this situation. In the **25-1S**/**25-4S** structure pair, the bridging ∠Fe-P-Fe angles are ~130°, which are larger than the usual 109° for the tetracoordinate phosphorus owing to the larger steric requirement for the Cp-Fe-PF_3 fragments relative to the fluorine atoms in the PF_2 group. In the **25-2S**/**25-3S** pair, the phosphorus is trigonal bipyramidally pentacoordinated with fluorine atoms in the axial positions with equatorial ∠Fe-P-Fe angles of about 145°. These are larger than the usual 120° for sp^2 hybridation, also attributed to a large steric effect. We tried to optimize other trigonal bipyramidal $Cp_2Fe_2(PF_3)_5$ structures with both Fe atoms on the axial positions (i.e., ∠Fe-P-Fe = 180°), but they eventually revert to structures **25-2S**/**25-3S**.

We have noted that the energy difference between the **25-1S**/**25-4S** *cis-trans* structure pair with bridging PF_2 groups (12.1 kcal/mol) is much larger than that between the *cis-trans* structure pair **25-2S**/**25-3S** with bridging PF_3 groups (9.7 – 7.5 = 2.2 kcal/mol). This may be attributed to different steric effects of the two Cp rings in these structures. Both *trans* structures **25-1S** and **25-2S**, present similar situations. In these structures the two Cp rings are widely separated with negligible steric effects since the smallest interring H···H distance is larger than 5.0 Å. However, in the *cis* structures **25-3S** and **25-4S**, the situations are different. In **25-3S** with a bridging PF_3 group the two Cp rings are only slightly closer than in the corresponding *trans* isomer with the smallest interring distance of 4.3 Å between the two Cp rings so that its energy is only 2.2 kcal/mol higher than that for **25-2S**. However, in the significantly higher energy *cis* structure **25-4S** with a bridging PF_2 group, the two Cp rings are much closer with the smallest interring H···H distance only ~2.5 Å. This steric effect can account for the

significantly higher energy of the *cis* isomer **25-4S** relative to the corresponding *trans* isomer **25-1S**.

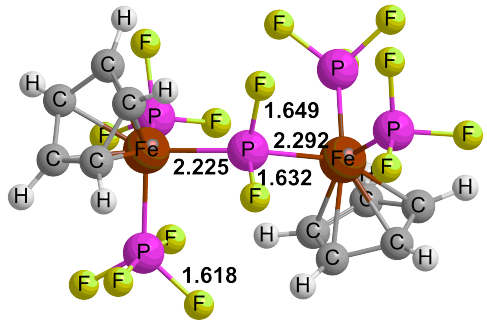

25-1S (C_1, 0.0, ∠Fe-P-Fe = 137.7)

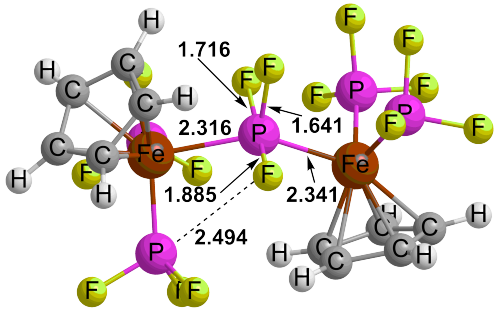

25-2S (C_1, 7.5, ∠Fe-P-Fe = 143.0)

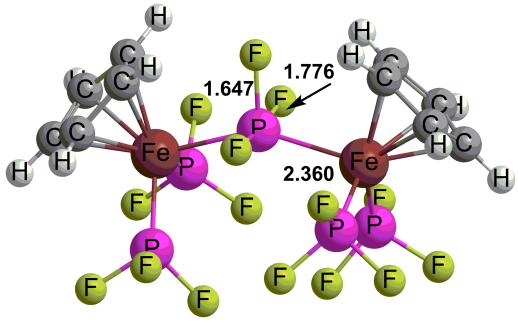

25-3S (C_2, 9.7, ∠Fe-P-Fe = 149.1)

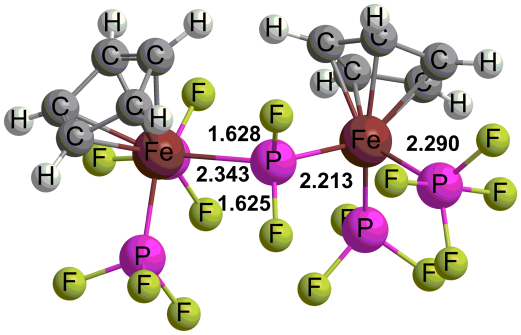

25-4S (C_1, 12.1, ∠Fe-P-Fe = 132.2)

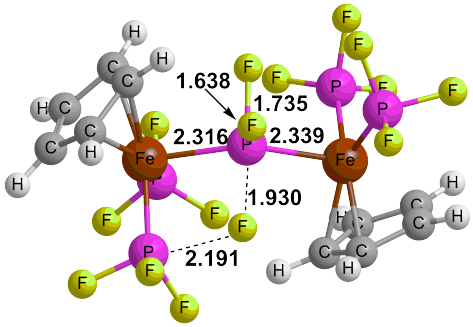

TS_{mig} (C_1, 7.5, ∠Fe-P-Fe = 141.5)

Figure 3. The optimized $Cp_2Fe_2(PF_3)_5$ structures, as well as the transition state structure TS_{mig} linking **25-1S** and **25-2S,** predicted by the B3LYP* method. The bond distances are in Å. The relative energies (kcal/mol) and the angles between the two Fe-P (bridging) bonds (degree) are also listed in the parentheses.

The bonds between the iron atoms and the bridging phosphorus atoms are formal single bonds, which give the each iron atom the favored 18-electron configuration. In this connection the bonds of the iron atoms to the bridging and terminal phosphorus atoms

have similar WBIs of 0.55 to 0.58 and 0.64 to 0.69, respectively. The slight difference in these WBIs can be attributed to the slightly longer bonds of the iron atoms (by ~0.2 Å) to the bridging phosphorus atoms relative to the terminal phosphorus atoms.

The lowest-lying *trans* structure $Cp_2Fe_2(PF_3)_3(PF_4)(\mu\text{-}PF_2)$ **25-1S** can be derived from **25-2S** by migration of a fluorine atom from the bridging PF_3 ligand to a terminal PF_3 ligand to give a bridging PF_2 group and a terminal PF_4 ligand. The activation barrier between **25-1S** and **25-2S** is critical, since it determines the kinetic stability of **25-2S**. In this connection, we have located the transition state $\mathbf{TS_{mig}}$ (Figure 3) between **25-2S** and **25-1S**, using intrinsic reaction coordinate (IRC) analysis to confirm that $\mathbf{TS_{mig}}$ connects **25-2S** and **25-1S**. Surprisingly, all three DFT methods predict the barrier from the **25-2S** side to be less than 0.4 kcal/mol (Table S19). This implies kinetic instability of **25-2S** so that only **25-1S** is likely to be accessible experimentally.

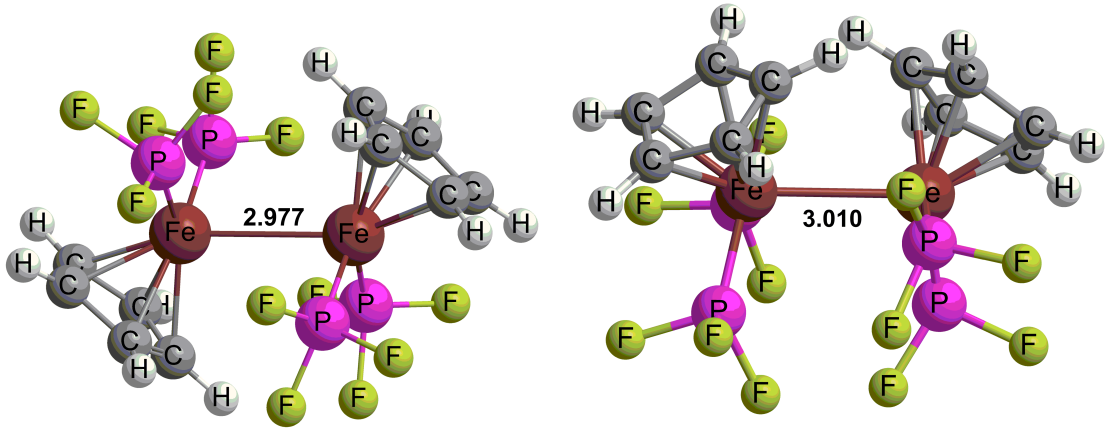

24-1S (C_2, 0.0) **24-2S (C_2, 5.1)**

Figure 4. The optimized $Cp_2Fe_2(PF_3)_4$ structures predicted by the B3LYP* method. The bond distances are in angstrom. The relative energies (kcal/mol) are listed in parentheses.

3.1.2 $Cp_2Fe_2(PF_3)_4$ Many kinds of starting structures have been tried for $Cp_2Fe_2(PF_3)_4$ including structures with all terminal PF_3 ligands, structures with two bridging PF_3 groups analogous to the $Cp_2Fe_2(\mu\text{-}CO)_2(CO)_2$ global minimum,[2,3,4,10] structures with two 4-electron donor bridging PF_3 groups analogous to the previously optimized C_{2h} $Fe_2(PF_3)_8$ structure,[35] and structures with two bridging Cp rings and four terminal PF_3 groups. However, a single structure type with all terminal PF_3 groups was found to lie at least 30 kcal/mol below isomeric $Cp_2Fe_2(PF_3)_4$ structures of any other type. Two such C_2 structures were found corresponding to a *cis*/*trans* isomer pair with the *trans* isomer **24-1S** lying 5.1 kcal/mol in energy below the *cis* isomer (Figure 4). Structure **24-1S** has a tiny imaginary frequency of 12*i* cm^{-1}, even using a finer integration grid.

However, a C_1 minimum has very small changes in both geometry (~0.01 Å) and energy (~1 kcal/mol). Thus the C_2 structure **24-1S** for $Cp_2Fe_2(PF_3)_4$ should be observed as an average geometry between two mirror image C_1 minima. The Fe–Fe distances of 2.977 Å for **24-1S** and 3.010 Å for **24-2S** can be interpreted as formal single bonds thereby giving each iron atom the favored 18-electron configuration. The higher energy and longer Fe–Fe distance in the *cis* isomer **24-2S** relative to the *trans* isomer **24-1S** can be related to the greater steric hindrance between the Cp rings in the former related to the latter.

Triplet $Cp_2Fe_2(PF_3)_4$ structures analogous to **24-1S** and **24-2S** were investigated using all three DFT methods but in all cases were found to dissociate into two individual $CpFe(PF_3)_2$ fragments.

3.1.3 $Cp_2Fe_2(PF_3)_3$. We attempted to optimize various types of structures for $Cp_2Fe_2(PF_3)_3$ with spin states ranging from singlet to nonet. However, all of the septet and nonet structures were found to be high energy structures, lying more than 20 kcal/mol in energy above the global minimum. Therefore, only low-lying singlet, triplet and quintet structures are considered in this paper. The lowest-lying $Cp_2Fe_2(PF_3)_3$ structure is the triplet structure **23-1T** (Figure 5). Another low-lying triplet structure **23-2T** (Figure 5) lies 5.8 kcal/mol above **23-1T**. These two unbridged asymmetrically coordinated triplet $Cp_2Fe_2(PF_3)_3$ structures correspond to a *cis*/*trans* isomer pair with the *trans* structure **23-1T** being the lower energy structure because of less steric hindrance between the Cp rings. In **23-1T** and **23-2T** the Fe–Fe bond distances of 2.675 and 2.796 Å, respectively, correspond to formal single bonds. The Mulliken spin densities of ~2.0 lie almost entirely on the iron atoms bearing only a single terminal PF_3 group as well as a Cp ring (the "left" iron atoms in Figure 5) corresponding to a high-spin 16-electron configuration for these iron atoms. The other iron atoms in **23-1T** and **23-2T**, bearing two terminal PF_3 groups as well as the Cp ring, have the favored 18-electron configuration.

A relatively low energy quintet $Cp_2Fe_2(PF_3)_3$ structure, **23-1Q**, lying only 3.4 kcal/mol above the triplet structure **23-1T**, is geometrically similar to that of the triplet structures **23-1T** and **23-2T**, but with a much shorter Fe-Fe distance of 2.444 Å (Figure 5). The Mulliken spin densities for the $CpFePF_3$ ("left") and the $CpFe(PF_3)_2$ ("right") Fe atoms are 3.39 and 0.29, respectively, indicating that the "left" Fe atom has at least three unpaired electrons, and the Fe-Fe bond is polarized.

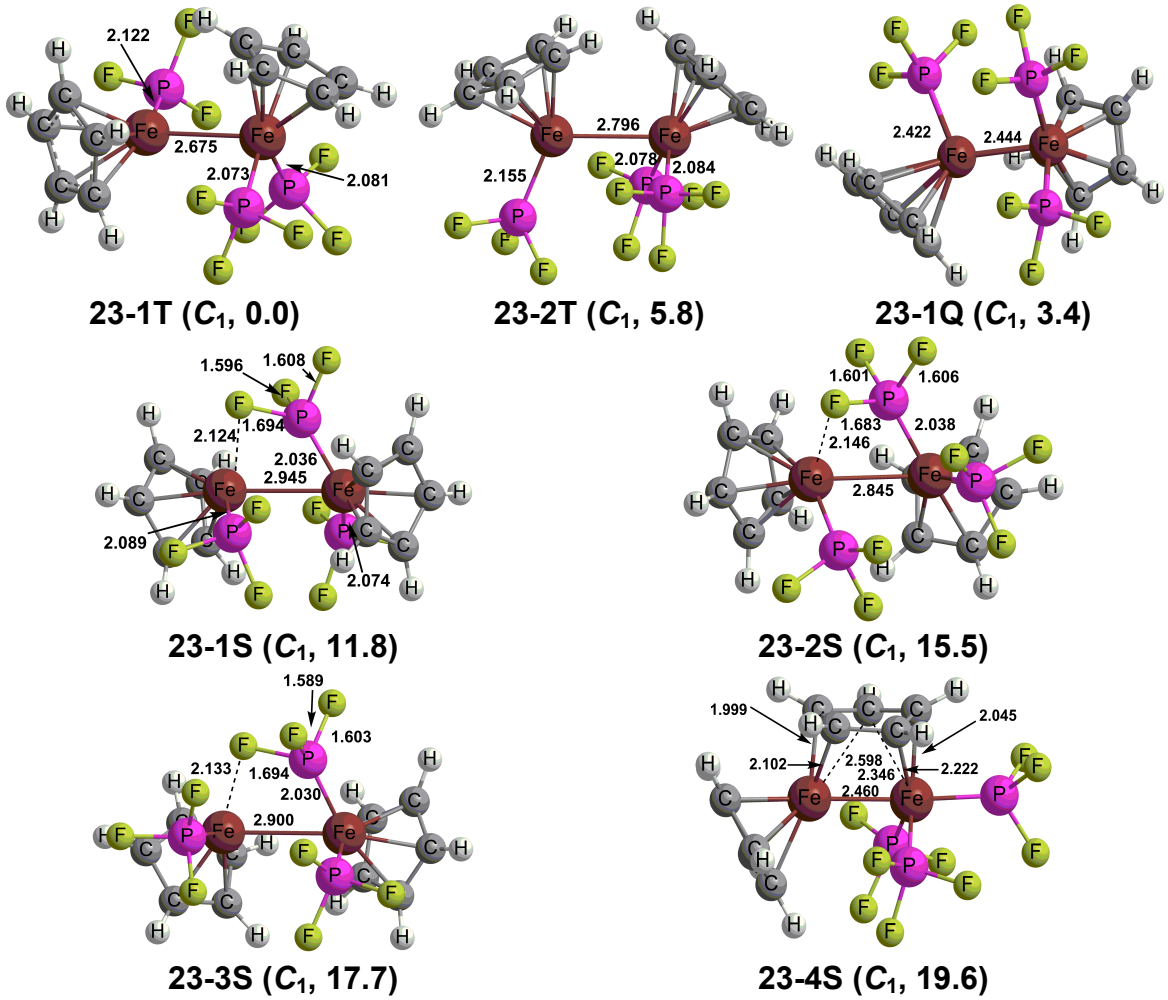

Figure 5. The optimized $Cp_2Fe_2(PF_3)_3$ structures predicted by the B3LYP* method. The bond distances are in Å. The relative energies (kcal/mol) are listed in parentheses.

The three lowest energy singlet $Cp_2Fe_2(PF_3)_3$ structures **23-1S**, **23-2S**, and **23-3S**, lying 11.8, 15.5, and 17.7 kcal/mol, respectively, above **23-1T**, have similar geometries with single unusual η^2-μ-PF_3 ligands bridging the two $CpFe(PF_3)$ fragments by forming both an Fe–P bond of length ~2.0 Å and an Fe–F bond of length ~2.1 Å (Figure 5). Such bridging η^2-μ-PF_3 groups exhibit low ν(PF) frequencies of 606, 621, and 609 cm^{-1}, respectively, for the P–F unit bridging the two iron atoms in **23-1S**, **23-2S**, and **23-3S** (Figure 5). These ν(PF) frequencies are significantly lower than those (750 to 860 cm^{-1}) for the nonbridging P-F units in these structures and those (810 to 840 cm^{-1}) for free isolated PF_3 at the same BP86/DZP level of theory (see Table S16 in Supporting Information). Bridging η^2-μ-PF_3 ligands of this type are four-electron donor ligands to the central Fe_2 system analogous to a four-electron bridging η^2-μ-CO group found in the

experimentally known species $(diphos)_2Mn_2(CO)_4(\eta^2\text{-}\mu\text{-}CO)$.[69,70] In an NBO analysis the second order perturbation of the Fock matrix is found from the filled orbitals of the fluorine atom to unoccupied orbitals of the iron atom. These bridging $\eta^2\text{-}\mu\text{-}PF_3$ groups thus donate two electrons to one iron atom through an F→Fe dative bond and two electrons to the other iron atom through a P→Fe dative bond. This is similar to the interactions between the F atom of the bridging CF_2 group and the Fe atom in a $Fe_2(CF_2)(CO)_5$ structure previously studied by DFT methods.[71] The Fe–Fe distances of 2.945, 2.845, and 2.900 Å in **23-1S**, **23-2S**, and **23-3S**, respectively, suggest formal single bonds, thereby giving each iron atom the favored 18-electron configuration. The only differences between the three structures **23-1S**, **23-2S**, and **23-3S** are the positions of the two terminal PF_3 groups relative to the four-electron donor bridging $\eta^2\text{-}\mu\text{-}PF_3$ group.

The fourth singlet $Cp_2Fe_2(PF_3)_3$ structure **23-4S**, lying 19.6 kcal/mol in energy above **23-1T**, has very different geometry from the previous three singlet structures **23-1S**, **23-2S**, and **23-3S** discussed above (Figure 5). Thus in **23-4S** all three PF_3 groups are bonded to the same iron atom (the "right" iron atom in Figure 5) and a terminal Cp ring is bonded to the other iron atom (the "left" iron atom in Figure 5). The other Cp ring bridges the Fe_2 bond by donating three electrons to the iron atom bearing the Cp ring and two electrons to the iron atom bearing the three PF_3 ligands. The Fe=Fe distance of 2.460 Å in **23-4S** is ~0.4 Å shorter than the Fe–Fe single bond distances in the three singlet structures **23-1S**, **23-2S**, and **23-3S** and thus can correspond to a formal double bond. This gives each iron atom in **23-4S** the favored 18-electron configuration.

3.1.4 $Cp_2Fe_2(PF_3)_2$. Six low-lying $Cp_2Fe_2(PF_3)_2$ structures were optimized, all of which are genuine minima with no imaginary vibrational frequencies (Figure 6). The lowest energy structure is an unbridged C_2 quintet spin state structure **22-1Q** with a small imaginary frequency of $11i$ cm^{-1}, which can be removed by using the finer (120,974) integration grid. Structure **22-1Q** consists of two $CpFe(PF_3)$ fragments linked by an Fe=Fe bond. The Fe=Fe distance of 2.322 Å suggests a formal double bond. The Mulliken spin densities of ~2.05 on each Fe atom show that each Fe atom has two unpaired electrons. One of these unpaired electrons on each iron can arise from a $\sigma + {}^2\!/_2\pi$ double bond with two orthogonal single electron π "half-bonds." Such an $\sigma + {}^2\!/_2\pi$ double bond in **22-1Q** is similar to that found in the experimentally known[5,6,7] and structurally characterized $Cp_2Fe_2(\mu\text{-}CO)_3$. An Fe=Fe double bond of any type in **22-1Q** gives each iron atom a 17-electron configuration leading to a second unpaired electron on each iron atom. This is consistent with the quintet spin state of **22-1Q**.

The lowest energy triplet $Cp_2Fe_2(PF_3)_2$ structure **22-1T**, lying only 0.3 kcal/mol above **22-1Q**, has both PF_3 ligands bonded as terminal ligands to the same iron atom (Figure 6). The short Fe=Fe distance of 2.310 Å in **22-1T** can correspond to a formal double bond. The Mulliken spin densities of ~2.0 for the iron atom bonded only to a Cp ring (the "left" iron atom in Figure 6) and ~0.0 for the iron atom bonded to two PF_3 groups in addition to a Cp ring (the "right" iron atom in Figure 6) suggest a 16-electron configuration for the former iron atom and an 18-electron configuration for the latter iron atom. This is consistent with a polarized Fe=Fe double bond between the iron atoms in **22-1T** with the iron atom bearing the PF_3 groups providing three electrons and the iron atom bearing only the Cp ring providing the fourth electron. The natural atomic charges of 0.66 and –0.71 for the iron atoms (Table 1) in **22-1T** are consistent with this polarization.

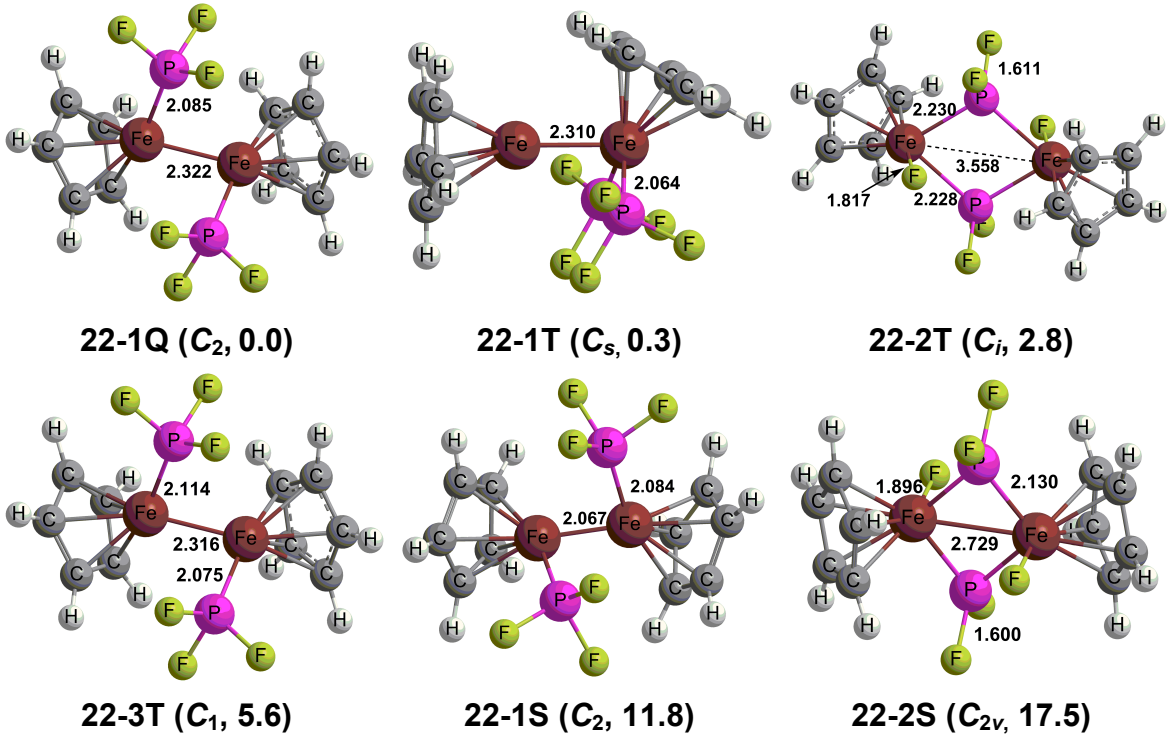

Figure 6. The optimized $Cp_2Fe_2(PF_3)_2$ structures predicted by the B3LYP* method. The bond distances are in Å. The relative energies (kcal/mol) are listed in the parentheses.

The triplet $Cp_2Fe_2(PF_3)_2$ structure **22-2T**, lying only 2.8 kcal/mol in energy above **22-1Q**, has a small imaginary frequency of 19*i* cm^{-1} (Figure 6). Following the corresponding normal mode leads to a C_1 structure with very little changes in geometry

and energy (~0.1 kcal/mol). In **22-2T**, both PF_3 ligands have fragment into bridging PF_2 groups and terminal fluorine atoms by rupture of one of the P–F bonds. Each bridging PF_2 ligand donates a single electron to one iron atom through a normal Fe–P covalent bond and two electrons to the other iron atom through a P→Fe dative bond. The Fe–F distances to the terminal fluorine atoms are 1.817 Å. The long Fe···Fe distance of 3.558 Å indicates the absence of a direct iron-iron bond. The Mulliken spin densities on the two Fe atoms are approximately unity, indicating that each Fe atom has one unpaired electron. This is consistent with a 17-electron count for each iron atom, consistent with a binuclear triplet.

The C_1 triplet $Cp_2Fe_2(PF_3)_2$ structure **22-3T**, lying 5.6 kcal/mol in energy above **22-1Q**, is geometrically similar to **22-1Q** (Figure 6). The Fe=Fe distance of 2.316 Å in **22-3T** is essentially identical to that of 2.322 Å in **22-2Q** and thus suggests a formal double bond. However, in **22-3T** this Fe=Fe double bond is a $\sigma + \pi$ double bond without any unpaired electrons contained in the bond rather than the $\sigma + {}^{2}\!/_{2}\pi$ double bond with two unpaired electrons within the bond suggested for **22-1Q**. The unequal Mulliken spin densities for the two Fe atoms in **22-3T** of 2.58 and –0.53 suggest a high-spin 16-electron configuration for one iron atom and an 18-electron configuration for the other iron atom rather than a 17-electron configuration for each iron atom.

Two low-lying singlet $Cp_2Fe_2(PF_3)_2$ structures were obtained (Figure 6). The unbridged C_2 structure **22-1S**, lying 11.8 kcal/mol in energy above **22-1Q**, has a very short Fe≡Fe distance of 2.067 Å with a correspondingly high WBI of 1.04 (Table 1). This is consistent with the formal triple bond required to give each iron atom the favored 18-electron configuration. The other singlet $Cp_2Fe_2(PF_3)_2$ structure, lying 17.5 kcal/mol in energy above **22-1Q**, is a doubly bridged C_{2h} structure **22-2S** geometrically similar to **22-2T** but with a much shorter Fe–Fe distance of 2.729 Å. This Fe–Fe distance coupled with an associated WBI of 0.26 (Table 1) suggests a formal single Fe-Fe bond thereby giving each iron atom in **22-2S** only a 16-electron configuration.

3.2 NBO analysis of the $Cp_2Fe_2(PF_3)_n$ Structures

The atomic charges on the two iron atoms and the Wiberg bond indices (WBIs) for the iron–iron bonds in the singlet $Cp_2Fe_2(PF_3)_n$ (n = 7, 6, 5) structures were obtained by NBO analysis (Table 1).[72,73,74] The natural atomic charges on a given iron atom are found to be related to the number of PF_3 ligands to which it is directly bonded. An increasing number of PF_3 groups leads to an increased natural negative charge. This suggests that electron-withdrawing properties of the three highly electronegative fluorines of the PF_3 group do not compensate fully for the negative charge on the iron

atom arising from the forward P→Fe σ bond from the PF_3 ligand. In the $Cp_2Fe_2(PF_3)_n$ structures with an unsymmetrical distribution of the PF_3 groups between the two iron atoms, such as the $Cp_2Fe_2(PF_3)_3$ structures **23-1S** to **23-4S**, the iron atom bearing more PF_3 groups has the larger negative charge.

Table 1. Atomic population, NBO analysis, and Fe-Fe bonding for the singlet $Cp_2Fe_2(PF_3)_n$ (n = 5, 4, 3, 2) structures by the B3LYP* method.

Structures	Natural charge on Fe/Fe	Wiberg bond index	Fe-Fe distance (Å)	Formal Fe-Fe bond order
25-1S	-0.64/-0.57	0.03	4.212	0
25-2S	-0.61/-0.58	0.03	4.416	0
25-3S	-0.60/-0.60	0.03	4.550	0
25-4S	-0.64/-0.59	0.04	4.165	0
24-1S	-0.53/-0.53	0.36	2.977	1
24-2S	-0.52/-0.52	0.37	3.010	1
23-1T	0.41/-0.61	0.32	2.675	1
23-2T	0.40/-0.54	0.28	2.796	1
23-1Q	0.83/-0.78	0.33	2.444	1
23-1S	0.00/-0.57	0.32	2.945	1
23-2S	0.01/-0.59	0.32	2.845	1
23-3S	0.02/-0.58	0.34	2.900	1
23-4S	0.23/-0.84	0.38	2.460	2
22-1Q	0.21/0.21	0.50	2.322	2
22-1T	0.66/-0.71	0.46	2.310	2
22-2T	0.28/0.28	0.06	3.558	0
22-3T	0.39/-0.06	0.50	2.316	2
22-1S	-0.18/-0.18	1.04	2.067	3
22-2S	-0.05/-0.05	0.25	2.729	1

The WBIs of the Fe-Fe bonds in the $Cp_2Fe_2(PF_3)_n$ structures (n = 5, 4, 3, 2) (Table 1) are relatively low for a given formal bond order owing to the role played by multicenter bonding in many of these highly bridged systems.[75,76] In addition, previous studies on the WBIs in metal–metal bonded derivatives suggest typical values of 0.2 to 0.3 for unbridged formal metal–metal single bonds.[77] For the $Cp_2Fe_2(PF_3)_n$ (n = 5, 4, 3, 2) structures, the relative WBI values, although much less than the absolute formal Fe–Fe bond orders, are nevertheless seen to correlate reasonably with the formal bond order assignments suggested by the Fe–Fe distances and electron counting (Table 1). Thus the formal Fe–Fe single bonds in the $Cp_2Fe_2(PF_3)_n$ (n = 4, 3, 2) derivatives have WBIs

ranging from 0.25 to 0.37. The WBIs for formal Fe=Fe double bonds are predicted to range from 0.38 to 0.50. The one example of a formal Fe≡Fe triple bond, namely that in **22-1S**, has an even higher WBI of 1.04. For those structures without direct Fe-Fe interaction, the WBIs are negligible, i.e., less than 0.06.

3.3 Thermochemistry of the $Cp_2Fe_2(PF_3)_n$ Structures

The $Cp_2Fe_2(PF_3)_n$ (n = 5, 4, 3, 2) species were evaluated with respect to their viabilities towards PF_3 dissociation, disproportionation into $Cp_2Fe_2(PF_3)_{n+1}$ + $Cp_2Fe_2(PF_3)_{n-1}$, and dissociation into mononuclear fragments (Table 2). All three $Cp_2Fe_2(PF_3)_n$ (n = 5, 4, 3) derivatives are seen to be viable with respect to PF_3 dissociation as indicated by substantial PF_3 dissociation energies of 23.1, 30.3, and 21.6 kcal/mol, respectively, for their lowest-lying singlet structures. These PF_3 dissociation energies are only slightly lower than the typical experimental bond energies D[$(CO)_{n-1}M$—CO] derived from the collision-induced dissociation threshold energies of 27, 41, and 37 kcal/mol for the simple binary metal carbonyls $Ni(CO)_4$, $Fe(CO)_5$, and $Cr(CO)_6$, respectively.[78] The relatively lower Gibbs free energies at 298.15 K (i.e., 11.1, 13.4, and 5.9 kcal/mol, respectively) suggest promotion these dissociation processes by the entropy contributions.

Although the $Cp_2Fe_2(PF_3)_n$ (n = 5, 4, 3, 2) species are viable with respect to PF_3 dissociation, the viability of $Cp_2Fe_2(PF_3)_n$ (n = 4, 3) towards disproportionation into $Cp_2Fe_2(PF_3)_{n+1}$ + $Cp_2Fe_2(PF_3)_{n-1}$ is limited. Thus the disproportionation of $Cp_2Fe_2(PF_3)_3$ into $Cp_2Fe_2(PF_3)_4$ + $Cp_2Fe_2(PF_3)_2$ is predicted to be exothermic but by only 8.7 kcal/mol (Table 2). The disproportionation of $Cp_2Fe_2(PF_3)_4$ into $Cp_2Fe_2(PF_3)_5$ + $Cp_2Fe_2(PF_3)_3$, although not exothermic, is endothermic by only 7.3 kcal/mol. This suggests that $Cp_2Fe_2(PF_3)_5$ is likely to be the most stable species. The Gibbs free energies of these disproportionation reactions (i.e., 2.3 and –7.5 kcal/mol) are qualitatively the same as the corresponding energies.

In order to study the thermochemistry of the dissociation reactions for the $Cp_2Fe_2(PF_3)_n$ structures into mononuclear fragments, the mononuclear $CpFe(PF_3)_n$ structures (n = 1, 2) were optimized (Figure 7). Considering only the lowest energy singlet binuclear $Cp_2Fe_2(PF_3)_n$ structures (n = 4, 3, 2) and doublet mononuclear $CpFe(PF_3)_n$ structures (n = 1, 2) structures leads to the dissociation energies in Table 2. The dissociation energy of the tetrakis(trifluorophosphine) complex $Cp_2Fe_2(PF_3)_4$ is predicted to be endothermic but with the relatively low dissociation energy of only 7.3 kcal/mol. This suggest that much of the chemistry of $Cp_2Fe_2(PF_3)_4$ might involve dissociation into such mononuclear $CpFe(PF_3)_2$ fragments, and the negative Gibbs free

energy, –15.3 kcal/mol, ensures the dissociation at room temperature. In contrast to $Cp_2Fe_2(PF_3)_4$, the energies for the dissociation of $Cp_2Fe_2(PF_3)_n$ (n = 3, 2) into mononuclear fragments are substantial at 23.5 and 48.4 kcal/mol, respectively. However, the corresponding Gibbs free energies including the entropy contribution at 298.15 K become lower by ~20 kcal/mol.

Table 2. The B3LYP* reaction energies without zero-point energy corrections (ΔE, kcal/mol) and related Gibbs free energies (ΔG_{298}, kcal/mol) for $Cp_2Fe_2(PF_3)_n$ (n = 5, 4, 3, 2) derivatives. All compounds are the lowest-lying minima.

Reaction	ΔE	ΔG
$Cp_2Fe_2(PF_3)_5 \rightarrow Cp_2Fe_2(PF_3)_4 + PF_3$	23.1	11.1
$Cp_2Fe_2(PF_3)_4 \rightarrow Cp_2Fe_2(PF_3)_3 + PF_3$	30.3	13.4
$Cp_2Fe_2(PF_3)_3 \rightarrow Cp_2Fe_2(PF_3)_2 + PF_3$	21.6	5.9
$2Cp_2Fe_2(PF_3)_4 \rightarrow Cp_2Fe_2(PF_3)_5 + Cp_2Fe_2(PF_3)_3$	7.3	2.3
$2Cp_2Fe_2(PF_3)_3 \rightarrow Cp_2Fe_2(PF_3)_4 + Cp_2Fe_2(PF_3)_2$	–8.7	–7.5
$Cp_2Fe_2(PF_3)_4 \rightarrow 2CpFe(PF_3)_2$	7.3	–15.3
$Cp_2Fe_2(PF_3)_3 \rightarrow CpFe(PF_3) + CpFe(PF_3)_2$	23.5	3.2
$Cp_2Fe_2(PF_3)_2 \rightarrow 2CpFe(PF_3)$	48.4	29.2
$2CpFe(PF_3)_2H \rightarrow Cp_2Fe_2(PF_3)_4 + H_2$	19.8	26.5
$2CpFe(CO)_2H \rightarrow Cp_2Fe_2(CO)_4 + H_2$	0.0	3.4
$Fe(PF_3)_5 + C_5H_6 \rightarrow C_5H_6Fe(PF_3)_3 + 2PF_3$	1.2	–10.8
$C_5H_6Fe(PF_3)_3 \rightarrow CpFe(PF_3)_2H + PF_3$	8.8	–5.5

The thermochemistry of the experimentally known reactions[39] $C_5H_6Fe(PF_3)_3 \rightarrow CpFe(PF_3)_2H + PF_3$ and $Fe(PF_3)_5 + C_5H_6 \rightarrow C_5H_6Fe(PF_3)_3 + 2PF_3$ was also investigated (Table 2). Both reactions are only slightly endothermic with enthalpies of 8.8 kcal/mol for the former and 1.2 kcal/mol for the latter (B3LYP*). However, the negative Gibbs free energies of –10.8 and –5.5 kcal/mol, respectively, for these reactions indicate that they are favored. Thus both reactions can be driven by the entropy effect as well as the escape of the volatile PF_3 product from the system. In addition, the substantial dissociation energy for the experimentally known hydride $CpFe(PF_3)_2H$ to $Cp_2Fe_2(PF_3)_4 + H_2$ of 19.8 kcal/mol (B3LYP*, Table 2) is consistent with the experimental isolation of $CpFe(PF_3)_2H$ as a stable compound. This contrasts with the carbonyl analogues for which the related reaction $2CpFe(CO)_2H \rightarrow Cp_2Fe_2(CO)_4 + H_2$ is predicted to be essentially thermoneutral (B3LYP*, Table 2). The latter is consistent with the instability of the hydride $CpFe(CO)_2H$. This is an example of the PF_3 derivative being more stable than its carbonyl analogue.

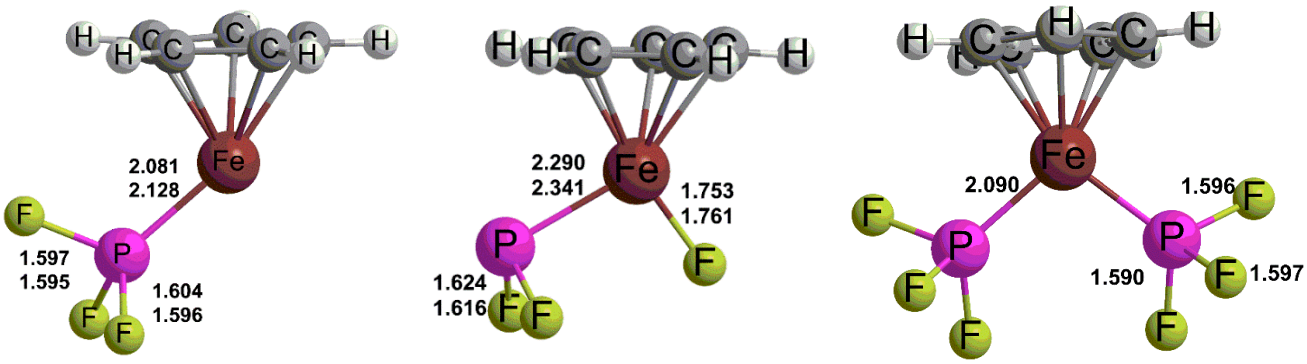

11-1 (C_s, D:18.8, Q: 0.0) **11-2 (C_s, D:21.8, Q: 6.5)** **12-1D (C_s, 0.0)**

Figure 7. The optimized $CpFe(PF_3)_n$ (n =1, 2) structures predicted by the B3LYP* method. The bond distances are in Å. The relative energies (kcal/mol) are listed in the parentheses. The bond distances for doublet (D) are on the top, while those for quartet (Q) are on the bottom.

4. Discussion

The $Cp_2Fe_2(CO)_n$ (n = 5, 4, 3, 2) system is characterized by the following features:

(1) The stable and experimentally known $Cp_2Fe_2(CO)_4$ and $Cp_2Fe_2(CO)_3$ structures have two and three bridging CO groups, respectively.

(2) The lowest energy predicted $Cp_2Fe_2(CO)_2$ structure has two bridging CO groups and probably is an intermediate in the pyrolysis of $Cp_2Fe_2(CO)_4$ to give $Cp_4Fe_4(CO)_4$.

(3) The pentacarbonyl $Cp_2Fe_2(CO)_5$ does not appear to be a viable compound.

The chemistry of the $Cp_2Fe_2(PF_3)_n$ (n = 5, 4, 3, 2) derivatives is totally different from that of the corresponding $Cp_2Fe_2(CO)_n$ derivatives, mainly because of the reluctance of PF_3 ligands to bridge iron-iron bonds analogous to the common type of bridging CO group. These structures are not similar to the known compounds[30,31] in which the PF_3 ligands act as μ_3 bridging groups bridging three rather than two metal atoms.

The pentakis(trifluorophosphine) complex $Cp_2Fe_2(PF_3)_5$ is predicted to be a viable compound in contrast to its carbonyl analogue $Cp_2Fe_2(CO)_5$, at least with respect to the obvious decomposition pathways. Most significantly, the PF_3 dissociation energy (~23 kcal/mol) and even the corresponding Gibbs free energy (~11 kcal/mol) of $Cp_2Fe_2(PF_3)_5$ to give $Cp_2Fe_2(PF_3)_4$ are considerable. The lowest energy $Cp_2Fe_2(PF_3)_5$ structure **25-1S** (Figure 3) is actually a *trans* $Cp_2Fe_2(PF_3)_3(PF_4)(\mu\text{-}PF_2)$ structure in which a fluorine atom migrates from one PF_3 ligand to another PF_3 ligand to give a bridging PF_2 group and a terminal PF_4 ligand with a very low activation barrier of less than 0.4 kcal/mol. Such kinetically favorable fluorine-migration processes may account for the

near absence of known compounds with bridging PF_3 groups. The *cis* $Cp_2Fe_2(PF_3)_3(PF_4)(\mu\text{-}PF_2)$ isomer **25-4S** corresponding to **25-1S** is found at significantly higher energies because of steric interference between the two Cp rings. The other type of low-energy $Cp_2Fe_2(PF_3)_5$ structures, namely the *cis*/*trans* isomer pair **25-2S** and **25-3S**, have a bridging PF_3 group but no Fe-Fe bonds. They can therefore be regarded as substitution products of a distorted trigonal bipyramidal PF_5 in which the axial fluorine atoms have been replaced by $CpFe(PF_3)_2$ moieties.

The unfavorability of PF_3 bridges across Fe-Fe bonds simplifies considerably the potential energy surface of $Cp_2Fe_2(PF_3)_4$ relative to its carbonyl analogue $Cp_2Fe_2(CO)_4$. Thus the *trans* and *cis* unbridged $Cp_2Fe_2(PF_3)_4$ structures **24-1S** and **24-2S**, respectively, lie more than 30 kcal/mol in energy below any other isomers.

The seven $Cp_2Fe_2(PF_3)_3$ structures lying within 20 kcal/mol of the lowest energy structure **23-1T** are of three different types (Figure 5). The triplet and quintet structures **23-1T**, **23-2T**, and **23-1Q** have exclusively terminal PF_3 groups. Their higher spin states reflect iron electron configurations less than the favored 18-electrons and/or $\sigma + {}^2\!/_2\pi$ formal Fe=Fe double bonds leading to two or four unpaired electrons for the triplets and quintets, respectively. An interesting feature of the three singlet $Cp_2Fe_2(PF_3)_3$ structures **23-1S**, **23-2S**, and **23-3S** is an unusual four-electron donor bridging η^2-μ-PF_3 group bonded to one iron atom through a P→Fe dative bond and to the other iron atom through an F→Fe dative bond. This type of η^2-μ-PF_3 group can bridge an Fe-Fe bond whereas a μ-PF_3 group using only its phosphorus atom to bridge an Fe-Fe bond appears to be highly disfavored. The other singlet $Cp_2Fe_2(PF_3)_3$ structure **23-4S** has three terminal PF_3 groups on one of the iron atoms and one of the Cp rings bridging the Fe-Fe bond.

The $Cp_2Fe_2(PF_3)_2$ energy surface includes six structures within 18 kcal/mol of the lowest energy structure **22-1Q** (Figure 6). Four of these structures (**22-1Q**, **22-1T, 22-3T**, and **22-1S**) have exclusively terminal PF_3 groups and spin states ranging from singlet to quintet. The singlet structure **22-1S** of this type has a short Fe≡Fe distance of ~2.07 Å consistent with the formal triple bond required to give each iron atom the favored 18-electron configuration. The remaining two low energy $Cp_2Fe_2(PF_3)_2$ structures **22-2T** and **22-2S** are actually $Cp_2Fe_2F_2(\mu\text{-}PF_2)_2$ structures with two terminal fluorine atoms and two bridging μ-PF_2 groups.

5. Conclusion

Theoretical studies on the binuclear $Cp_2Fe_2(PF_3)_n$ (n = 4, 3, 2) derivatives indicate the absence of low-energy structures having PF_3 ligands bridging Fe-Fe bonds. This contrasts with the analogous $Cp_2Fe_2(CO)_n$ systems for which the lowest energy structures have two (for n = 4 and 2) or three (for n = 3) CO groups bridging an iron-iron bond. However, higher energy singlet $Cp_2Fe_2(PF_3)_3$ structures have a novel four-electron donor bridging η^2-μ-PF_3 ligand bonded to one iron atom through its phosphorus atom and to the other iron atom through a fluorine atom. Other higher energy triplet and singlet $Cp_2Fe_2(PF_3)_2$ structures are of the $Cp_2Fe_2F_2(\mu\text{-}PF_2)_2$ type with terminal fluorine atoms and bridging μ-PF_2 ligands.

Although $Cp_2Fe_2(CO)_5$ is unknown, the trifluorophosphine analogue $Cp_2Fe_2(PF_3)_5$ is predicted to be a viable species. The lowest energy $Cp_2Fe_2(PF_3)_5$ structure is actually $Cp_2Fe_2(PF_3)_3(PF_4)(\mu\text{-}PF_2)$ with a bridging PF_2 group and a terminal PF_4 group. Such structures are derived from a $Cp_2Fe_2(PF_3)_4(\mu\text{-}PF_3)$ precursor by migration of a fluorine atom from the bridging PF_3 group to a terminal PF_3 group with a low activation energy barrier. Fluorine migration processes of this type might account for the absence of known compounds with PF_3 groups bridging a pair of metal atoms.

Acknowledgments We are indebted to the National Natural Science Foundation of China (21273082), the Scientific Research Foundation of Graduate School of South China Normal University (2013kyjj008), and the U. S. National Science Foundation (Grants CHE-1057466 and CHE-1361178) for support of this research.

Electronic supplementary information (ESI) available: Figure S1-S4. The optimized geometries (distances in Å) and the relative energies (kcal/mol) of the $Cp_2Fe_2(PF_3)_n$ (n = 5, 4, 3, 2) structures by the B3LYP, the BP86, and the B3LYP* method. Figure S5. The optimized geometries (distances in Å) and the relative energies (kcal/mol) of the $CpFe(PF_3)_n$ (n = 2, 1) structures by the B3LYP, the BP86, and the B3LYP* method. Tables S1 to S2. Atomic population, NBO analysis, and Fe-Fe bonding for the singlet $Cp_2Fe_2(PF_3)_n$ (n = 5, 4, 3, 2) structures. Table S3. Reaction energies (in kcal/mol) for some reactions of $Cp_2Fe_2(PF_3)_n$ (n = 5, 4, 3, 2) derivatives by three methods. Table S4-S15. Harmonic vibrational frequencies (cm^{-1}) and corresponding infrared intensities (km/mol, in parentheses) predicted for the $Cp_2Fe_2(PF_3)_n$ (n = 5, 4, 3, 2) structures. Table S16. Harmonic vibrational frequencies (cm^{-1}) and corresponding infrared intensities (km/mol, in parentheses) predicted for the isolated PF_3 structures. Table S17-S36. Cartesian coordinates and energies for the $Cp_2Fe_2(PF_3)_n$ (n = 5, 4, 3, 2) structures. Table S37-S41. Cartesian coordinates (Å) and energies (in hartree) for the $CpFe(PF_3)_n$ (n = 2, 1) structures.

Literature References

(1) Piper, T. S.; Wilkinson, G. *J. Inorg. Nucl. Chem.* **1956**, *6*, 104.
(2) Mills, O. S. *Acta Cryst*. **1958**, *11*, 620.
(3) Bryan, R. F.; Greene, P. T. *J. Chem. Soc. A* **1970**, 3068.
(4) Mitschler, A.; Rees, B.; Lehmann, M. S. *J. Am. Chem. Soc.* **1978**, *100*, 3390.
(5) Caspar, J. V.; Meyer, T. J. *J. Am. Chem. Soc.* **1980**, *102*, 7794.
(6) Hooker, R. H.; Mahmoud, K. A.; Rest, A. J. *Chem. Commun.* **1983**, 1022.
(7) Hepp, A. F.; Blaha, J. P.; Lewis, C.; Wrighton, M. S. *Organometallics* **1984**, *3*, 174.
(8) Blaha, J. P.; Bursten, B. E.; Dewan, J. C.; Frankel, R. B.; Randolph, C. L.; Wilson, B. A.; Wrighton, M. S. *J. Am. Chem. Soc.* **1985**, *1076*, 4561.
(9) Vitale, M.; Archer, M. E.; Bursten, B. E. *Chem. Commun*. **1998**, 179.
(10) Wang, H. Y.; Xie, Y.; King, R. B.; Schaefer, H. F. *Inorg. Chem.* **2006**, *45*, 3384.
(11) King, R. B. *Inorg. Chem.* **1966**, *5*, 2227.
(12) Green, J. C.; King, D. I.; Eland. J. H. D. *J. Chem. Soc. D* **1970**, 1121.
(13) Hillier, I. H.; Saunders, V. R.; Ware, M. J.; Bassett, P. J.; Lloyd, D. R.; Lynaugh, N. *Chem. Comm.* **1970**, 1316.
(14) Bassett, P. J.; Higginson, B. R.; Lloyd, D. R.; Lynaugh, N.; Roberts, P. J. *J. Chem. Soc. Dalton* **1974**, 2316.
(15) Müller, J.; Fenderl, K.; Mertschenk, B. *Chem. Ber.* **1971**, *104*, 700.
(16) Head, R. A.; Nixon, J. F.; Sharp, G. J.; Clark, R. J. *J. Chem. Soc. Dalton* **1975**, 2054.
(17) Nixon, J. F.; Seddon, E. A.; Suffolk, R. J.; Taylor, M. J.; Green, J. C.; Clark, R. J. *J. Chem. Soc. Dalton* **1986**, 765.
(18) Savariault, J.-M.; Serafini, A.; Pellissier, M.; Cassoux, P. *Theor. Chim. Acta* **1976**, *42*, 155.
(19) Braga, M. *Inorg. Chem.* **1985**, *24*, 2702.
(20) Braga, M. *J. Mol Struct.* **1992**, *85*, 167.
(21) Frenking, G.; Wichmann, K.; Fröhlich, N.; Grobe, J.; Golla, W.; Le Van, D.; Krebs, B.; Läge, M. *Organometallics* **2002**, *21*, 2921.
(22) Irvine, J. W.; Wilkinson, G. *Science* **1951**, *113*, 742.
(23) Wilkinson, G. *J. Am. Chem. Soc.* **1951**, *73*, 5501.
(24) Kruck, T. *Angew. Chem. Int. Ed.* **1967**, *6*, 53.
(25) Kruck, T. *Z. Naturforsch.* **1964**, *19*, 164.

(26) Kruck, T.; Baur. K. *Angew. Chem.* **1965**. *77*, 505.
(27) Kruck, T., K. Baur. *Z. Anorg. Allg. Chem.* **1969**, *364*, 192.
(28) Bennett, M. A.; Johnson, R. N.; Turney T. W. *Inorg. Chem.* **1976**, *15*, 2938.
(29) Drews, T.; Rusch, D.; Seidel, S.; Willemsen, S.; Seppelt, K. *Chem. Eur. J.* **2008**, *14*, 4280.
(30) Balch, A. L.; Davis, B. J.; Olmstead, M. M. *J. Am. Chem. Soc.* **1990**, *112*, 8593.
(31) Balch, A. L.; Davis, B. J.; Olmstead, M. M. *Inorg. Chem.* **1993**, *32*, 3937.
(32) Pechmann, T.; Brandt, C. D.; Werner, H. *Angew. Chem. Int. Ed.* **2000**, *39*, 3909.
(33) Pechmann, T.; Brandt, C. D.; Röger, C.; Werner, H. *Angew. Chem. Int. Ed.* **2000**, *39*, 3909.
(34) Pechmann, T.; Brandt, C. D.; Werner, H. *Dalton Trans.* **2004**, 959.
(35) Zou, R.; Li, Q.-s.; Xie, Y.; King, R. B.; Schaefer, H. F. *Chem. Eur. J.* **2008,** *14*, 11149.
(36) Yang, H.-q.; Li, Q.-s.; Xie, Y.; King, R. B.; Schaefer, H. F. *Mol. Phys.* **2010**, *108*, 2477.
(37) Yang, H.-q.; Li, Q.-s.; Xie, Y.; King, R. B.; Schaefer, H. F. *J. Phys. Chem. A* **2010**, *114*, 8896
(38) Gong, S.; Wang, C.; Li, Q.-s.; Xie, Y.; King, R. B. *J. Coord. Chem.* **2012**, *65*, 14.
(39) Kruck, T., Knoll, L. *Chem. Ber.* **1972**, *105*, 3783.
(40) Ziegler T.; Autschbach, J. *Chem. Rev.* **2005**, *105*, 2695.
(41) Bühl, M.; Kabrede, H. *J. Chem. Theory Comput.* **2006**, *2*, 1282.
(42) Brynda, M.; Gagliardi, L.; Widmark, P. O.; Power, P. P.; Roos, B. O. *Angew. Chem. Int. Ed.* **2006**, *45*, 3804.
(43) Sieffert, N.; Bühl, M. *J. Am. Chem. Soc.* **2010**, *132*, 8056.
(44) Schyman, P.; Lai, W.; Chen, H.; Wang, Y.; Shaik, S. *J. Am. Chem. Soc.* **2011**, *133*, 7977.
(45) Adams, R. D.; Pearl, W. C.; Wong, Y. O.; Zhang, Q.; Hall, M. B.; Walensky, J. R. *J. Am. Chem. Soc.* **2011**, *133*, 12994.
(46) Lonsdale, R.; Olah, J.; Mulholland, A. J.; Harvey, J. A. *J. Am. Chem. Soc.* **2011**, *133*, 15464.
(47) Becke, A. D. *J. Chem. Phys.* **1993**, *98*, 5648.
(48) Lee, C.; Yang, W.; Parr, R. G. *Phys. Rev. B* **1988**, *37*, 785.
(49) Becke, A. D. *Phys. Rev. A* **1988**, *38*, 3098.
(50) Perdew, J. P. *Phys. Rev. B* **1986**, *33*, 8822.
(51) Reiher, M.; Salomon, O.; Hess, B. A. *Theor. Chem. Acc.* **2001**, *107*, 48.

(52) Kepp, K. P. *Coord. Chem. Rev.* **2013**, *257*, 196.
(53) Houghton, B. J.; Deeth, R. J. *Eur. J. Inorg. Chem.* **2014**, 4573.
(54) Swart, M. *J. Chem. Theory Comput.* **2008**, *4*, 2057.
(55) Hughes, T. F.; Friesner, R. A. *J. Chem. Theory Comput.* **2011**, *7*, 19.
(56) Daku, L. M. L.; Aquilante, F.; Robinson, T. W.; Hauser, A. *J. Chem. Theory Comput.* **2012**, *8*, 4216.
(57) Salomon, O.; Reiher, M.; Hess, B. A. *J. Chem. Phys.* **2002**, *117*, 4729.
(58) Dunning, T. H. *J. Chem. Phys*. **1970**, *53*, 2823.
(59) Dunning, T. H.; Hay, P. J. In *Methods of Electronic Structure Theory*; Schaefer, H. F., Ed; Plenum, New York, 1977, pp. 1–27.
(60) Wachters, A. J. H. *J. Chem. Phys.* **1970**, *52*, 1033.
(61) Hood, D. M.; Pitzer, R. M.; Schaefer, H. F. *J. Chem. Phys.* **1979**, *71*, 705.
(62) Frisch, M. J.; Trucks, G. W.; Schlegel, H. B.; Scuseria, G. E.; Robb, M. A.; Cheeseman, J. R.; Scalmani, G.; Barone, V.; Mennucci, B.; Petersson, G. A.; Nakatsuji, H.; Caricato, M.; Li, X.; Hratchian, H. P.; Izmaylov, A. F.; Bloino, J.; Zheng, G.; Sonnenberg, J. L.; Hada, M.; Ehara, M.; Toyota, K.; Fukuda, R.; Hasegawa, J.; Ishida, M.; Nakajima, T.; Honda, Y.; Kitao, O.; Nakai, H.; Vreven, T.; Montgomery, J. A., Jr.; Peralta, J. E.; Ogliaro, F.; Bearpark, M.; Heyd, J. J.; Brothers, E.; Kudin, K. N.; Staroverov, V. N.; Kobayashi, R.; Normand, J.; Raghavachari, K.; Rendell, A.; Burant, J. C.; Iyengar, S. S.; Tomasi, J.; Cossi, M.; Rega, N.; Millam, M. J.; Klene, M.; Knox, J. E.; Cross, J. B.; Bakken, V.; Adamo, C.; Jaramillo, J.; Gomperts, R.; Stratmann, R. E.; Yazyev, O.; Austin, A. J.; Cammi, R.; Pomelli, C.; Ochterski, J. W.; Martin, R. L.; Morokuma, K.; Zakrzewski, V. G.; Voth, G. A.; Salvador, P.; Dannenberg, J. J.; Dapprich, S.; Daniels, A. D.; Farkas, Ö.; Foresman, J. B.; Ortiz, J. V.; Cioslowski, J.; Fox, D. J. Gaussian 09, Revision B.01; Gaussian, Inc., Wallingford CT, **2010**.
(63) Frisch, M. J.; Trucks, G. W.; Schlegel, H. B.; Scuseria, G. E.; Robb, M. A.; Cheeseman, J. R.; Montgomery, Jr., J. A.; Vreven, T.; Kudin, K. N.; Burant, J. C.; Millam, J. M.; Iyengar, S. S.; Tomasi, J.; Barone, V.; Mennucci, B.; Cossi, M.; Scalmani, G.; Rega, N.; Petersson, G. A.; Nakatsuji, H.; Hada, M.; Ehara, M.; Toyota, K.; Fukuda, R.; Hasegawa, J.; Ishida, M.; Nakajima, T.; Honda, Y.; Kitao, O.; Nakai, H.; Klene, M.; Li, X.; Knox, J. E.; Hratchian, H. P.; Cross, J. B.; Bakken, V.; Adamo, C.; Jaramillo, J.; Gomperts, R.; Stratmann, R. E.; Yazyev, O.; Austin, A. J.; Cammi, R.; Pomelli, C.; Ochterski, J. W.; Ayala, P. Y.; Morokuma, K.; Voth, G. A.; Salvador, P.; Dannenberg, J. J.; Zakrzewski, V. G.; Dapprich, S.;

Daniels, A. D.; Strain, M. C.; Farkas, O.; Malick, D. K.; Rabuck, A. D.; Raghavachari, K.; Foresman, J. B.; Ortiz, J. V.; Cui, Q.; Baboul, A. G.; Clifford, S.; Cioslowski, J.; Stefanov, B. B.; Liu, G.; Liashenko, A.; Piskorz, P.; Komaromi, I.; Martin, R. L.; Fox, D. J.; Keith, T.; Al-Laham, M. A.; Peng, C. Y.; Nanayakkara, A.; Challacombe, M.; Gill, P. M. W.; Johnson, B.; Chen, W.; Wong, M. W.; Gonzalez, C.; and Pople, J. A. Gaussian 03, Revision C.02; Gaussian, Inc., Wallingford CT, **2004**.

(64) Papas, B. N.; Schaefer, H. F. *J. Mol. Struct.* **2006**, *768*, 175.

(65) Jacobsen, H.; Ziegler, T. *J. Am. Chem.* Soc. **1996**, *118*, 4631.

(66) Martin, J. M. L.; Bauschlicher, C. W.; Ricca, A. *Comput. Phys. Commun*. **2001**, *133*, 189.

(67) Jonas, V.; Thiel, W. *J. Chem. Phys*. **1995**, *102*, 8474.

(68) Silaghi-Dumitrescu, I.; Bitterwolf, T. E.; King, R. B. *J. Am. Chem. Soc.* **2006**, *128*, 5342.

(69) Colton, R.; Commons, C. J. *Aust. J. Chem.* **1975**, *28*, 1673.

(70) Commons, C. J.; Hoskins, B. F. *Aust. J. Chem.* **1975**, *28*, 1663.

(71) Gong, S.; Wu, Y.; Li, Q.-s.; Xie, Y.; King, R. B. *J. Fluorine Chem.* **2013**, *151*, 12.

(72) NBO 5.0. Glendening, E. D.; Badenhoop, J, K.; Reed, A. E.; Carpenter, J. E.; Bohmann, J. A.; Morales, C. M.; Weinhold, F. Theoretical Chemistry Institute, University of Wisconsin, Madison (2001).

(73) Reed, A. E.; Curtiss, L. A.; Weinhold, F. *Chem. Rev.* **1988**, *88*, 899.

(74) Wiberg, K. B. *Tetrahedron* **1968**, *24*, 1083.

(75) Ponec, R.; Lendvay, G.; Chaves, J. *J. Comput. Chem.* **2008**, *29*, 1387.

(76) Green, J. C.; Green, M. L. H.; Parkin, G. *Chem. Commun.* **2012**, *48*, 11481.

(77) Xie, Y.; Schaefer, H. F.; King, R. B. *J. Am. Chem. Soc.* **2000**, *122*, 8746.

(78) Sunderlin, L. S.; Wang, D.; Squires, R. R. *J. Am. Chem. Soc.* **1993**, *115*, 12060.